New Day in Medicine
Новый День в Медицине
NDM

TIBBIYOTDA YANGI KUN

Ilmiy referativ, marifiy-ma'naviy jurnal

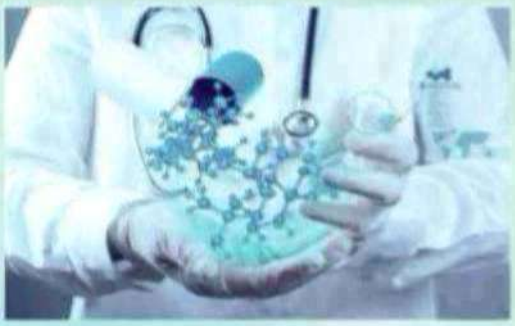

AVICENNA-MED.UZ

ISSN 2181-712X.
EiSSN 2181-2187

8 (94) 2026

ТИББИЁТДА ЯНГИ КУН
НОВЫЙ ДЕНЬ В МЕДИЦИНЕ
NEW DAY IN MEDICINE

Илмий-рефератив, маънавий-маърифий журнал
Научно-реферативный,
духовно-просветительский журнал

УЧРЕДИТЕЛИ:

БУХАРСКИЙ ГОСУДАРСТВЕННЫЙ МЕДИЦИНСКИЙ ИНСТИТУТ
ООО «ТИББИЁТДА ЯНГИ КУН»

Национальный медицинский исследовательский центр хирургии имени А.В. Вишневского является генеральным научно-практическим консультантом редакции

Журнал был включен в список журнальных изданий, рецензируемых Высшей Аттестационной Комиссией Республики Узбекистан (Протокол № 201/03 от 30.12.2013 г.)

8 (94)

2026

Август

www.bsmi.uz
https://newdaymedicine.com
E: ndmuz@mail.ru
Тел: +99890 8061882

Received: 20.07.2026, Accepted: 06.08.2026, Published: 10.08.2026

UDC 616.24-091.8:615.917-099-036.11

MORPHOLOGICAL FEATURES OF PULMONARY COMPLICATIONS AFTER ACUTE CARBON MONOXIDE POISONING: A LITERATURE REVIEW

Fayziyev Yusufjon Qadirovich https://orcid.org/0009-0007-6512-8055
e-mail: fayziyevyusuf590@gmail.com
Qurbonov Obid Maxsudovich https://orcid.org/0000-0001-7158-7038
e-mail: obidkurbanov61@gmail.com

Bukhara State Medical Institute named after Abu Ali ibn Sina, Uzbekistan, Bukhara, st. A. Navoi. 1
Tel: +998 (65) 223-00-50 e-mail: info@bsmi.uz

✓ ***Resume***

Background. Acute carbon monoxide (CO) poisoning remains one of the commonest lethal chemical injuries worldwide, accounting for an estimated 28 900 unintentional deaths and 1.18 million years of life lost in 2021. Although the brain and the myocardium dominate the clinical literature, the lung is simultaneously the portal of entry, the organ of elimination and a target tissue, and the morphology of CO-induced pulmonary injury remains comparatively poorly systematised. Objective. To synthesise the evidence published over the last decade on the macroscopic, microscopic, morphometric, histochemical and immunohistochemical features of pulmonary complications after acute CO poisoning and to define the structural correlates of their clinical phenotypes. Methods. A narrative review was performed in PubMed/MEDLINE, Scopus, Web of Science, Google Scholar and eLIBRARY for the period 2015–2026, complemented by seminal earlier work. Fifty sources - clinical cohorts, forensic autopsy series, rodent inhalational models and diagnostic syntheses - were analysed and organised by level of biological organisation and by time after exposure. Results. The evidence describes a reproducible two-phase trajectory. An early vascular–exudative phase (microcirculatory congestion and stasis, increased alveolar–capillary permeability, interstitial and alveolar oedema, diapedetic haemorrhage, bronchiolar epithelial desquamation) is followed, in survivors, by a delayed phase in which macrophage-driven inflammation, apoptosis, extracellular-matrix remodelling, emphysematous alveolar destruction and focal fibrosis predominate. Pulmonary oedema (80%), emphysematous change (42%) and haemorrhage (27%) are the commonest autopsy findings, and they correlate poorly with blood carboxyhaemoglobin. Morphometry and the paired markers CD68 and caspase-3 quantify the two components; age markedly modifies both severity and reversibility. Conclusion. CO-induced lung injury is a staged, quantifiable morphological process; combined morphometric and immunohistochemical assessment should be standardised for diagnostic, forensic and experimental use.

Keywords: carbon monoxide poisoning; lung; alveolar damage; pulmonary oedema; emphysema; morphometry; CD68; caspase-3; immunohistochemistry; forensic pathology.

O‘TKIR IS GAZI BILAN ZAHARLANISHDAN KEYINGI O‘PKA ASORATLARINING MORFOLOGIK XUSUSIYATLARI: ADABIYOTLAR SHARHI

Fayziyev Yusufjon Qadirovich https://orcid.org/0009-0007-6512-8055
e-mail: fayziyevyusuf590@gmail.com
Qurbonov Obid Maxsudovich https://orcid.org/0000-0001-7158-7038
e-mail: obidkurbanov61@gmail.com

Abu Ali ibn Sino nomidagi Buxoro davlat tibbiyot instituti, O‘zbekiston, Buxoro sh. A. Navoiy kochasi 1 Tel: +998 (65) 223-00-50 e-mail: info@bsmi.uz

✓ ***Rezyume***

Dolzarbligi. O‘tkir is gazi (uglerod oksidi, CO) bilan zaharlanish dunyoda eng ko‘p uchraydigan va o‘limga olib keluvchi kimyoviy shikastlanishlardan biri bo‘lib qolmoqda: 2021-yilda tasodifiy zaharlanish oqibatida 28 900 ta o‘lim va 1,18 mln yo‘qotilgan hayot yili qayd etilgan. Adabiyotlarda asosan bosh miya va miokard shikastlanishi yoritilgan bo‘lsa-da, o‘pka bir vaqtning o‘zida zaharning kirish darvozasi, chiqarilish a’zosi va nishon to‘qima hisoblanadi; uning morfologik o‘zgarishlari esa yetarlicha tizimlashtirilmagan. Maqsad. So‘nggi o‘n yillikda chop etilgan ma’lumotlar asosida o‘tkir is gazi bilan zaharlanishdan keyingi o‘pka asoratlarining makroskopik, mikroskopik, morfometrik, gistokimyoviy va immunogistokimyoviy xususiyatlarini umumlashtirish. Usullar. PubMed/MEDLINE, Scopus, Web of Science, Google Scholar va eLIBRARY bazalarida 2015–2026-yillar uchun tavsiflovchi (narrativ) sharh o‘tkazildi; tahlilga 50 ta manba — klinik kuzatuvlar, sud-tibbiy autopsiya seriyalari, kalamushlarda inhalatsion modellar va diagnostik sharhlar kiritildi. Natijalar. Ma’lumotlar ikki bosqichli qonuniy dinamikani ko‘rsatadi: erta vaskulyar-ekssudativ bosqich (mikrosirkulyator to‘laqonlik va staz, alveolyar-kapillyar o‘tkazuvchanlikning ortishi, interstitsial va alveolyar shish, diapedez qon quyilishlar, bronxiolalar epiteliysining ko‘chishi) hamda kechki bosqich (makrofagal yallig‘lanish, apoptoz, hujayralararo matriksning qayta qurilishi, emfizematoz destruksiya va o‘choqli fibroz). Autopsiyada eng ko‘p o‘pka shishi (80%), emfizematoz o‘zgarishlar (42%) va qon quyilishlar (27%) aniqlanadi; ular karboksigemoglobin darajasi bilan korrelyatsiyalanmaydi. CD68 va Caspase-3 markerlari hamda morfometriya ushbu ikki komponentni miqdoriy baholash imkonini beradi; yosh omili og‘irlik va qaytuvchanlikni belgilaydi. Xulosa. Is gazi ta’siridagi o‘pka shikastlanishi bosqichli va miqdoriy baholanadigan morfologik jarayon bo‘lib, morfometrik va immunogistokimyoviy tekshiruvlarni birgalikda standartlashtirish zarur.

Kalit so‘zlar: is gazi bilan zaharlanish; o‘pka; alveolyar shikastlanish; o‘pka shishi; emfizema; morfometriya; CD68; Caspase-3; immunogistokimyo; sud tibbiyoti.

МОРФОЛОГИЧЕСКИЕ ОСОБЕННОСТИ ЛЁГОЧНЫХ ОСЛОЖНЕНИЙ ПОСЛЕ ОСТРОГО ОТРАВЛЕНИЯ УГАРНЫМ ГАЗОМ: ОБЗОР ЛИТЕРАТУРЫ

Файзиев Юсуфжон Кадирович https://orcid.org/0009-0007-6512-8055
e-mail: fayziyevyusuf590@gmail.com
Курбанов Обид Махсудович https://orcid.org/0000-0001-7158-7038
e-mail: obidkurbanov61@gmail.com

Бухарский государственный медицинский институт имени Абу Али ибн Сины, Узбекистан, г. Бухара, ул. А. Навои. 1 Тел: +998 (65) 223-00-50 e-mail: info@bsmi.uz

✓ ***Резюме***

Актуальность. Острое отравление угарным газом (CO) остаётся одним из самых частых смертельных химических поражений: в 2021 г. в мире зарегистрировано 28 900 случаев смерти и 1,18 млн потерянных лет жизни. Несмотря на доминирование в литературе церебральных и кардиальных поражений, лёгкие являются одновременно входными воротами, органом элиминации и органом-мишенью, а их морфология систематизирована недостаточно. Цель. Обобщить данные последнего десятилетия о макро-, микроскопических, морфометрических, гистохимических и иммуногистохимических особенностях лёгочных осложнений острого отравления CO. Материал и методы. Нарративный обзор по базам PubMed/MEDLINE, Scopus, Web of Science, Google Scholar и eLIBRARY за 2015–2026 гг.; проанализировано 50 источников — клинические когорты, судебно-медицинские серии вскрытий, экспериментальные ингаляционные модели и диагностические обзоры. Результаты. Данные описывают двухфазную динамику: раннюю сосудисто-экссудативную фазу (полнокровие и стаз, повышение проницаемости аэрогематического барьера, интерстициальный и альвеолярный отёк, диапедезные кровоизлияния, десквамация бронхиолярного эпителия) и позднюю фазу (макрофагальное воспаление, апоптоз, ремоделирование матрикса, эмфизема и очаговый фиброз). На вскрытии чаще всего выявляются отёк (80%), эмфизематозные изменения (42%) и кровоизлияния (27%), не коррелирующие с уровнем карбоксигемоглобина. Заключение. Поражение лёгких при отравлении CO — стадийный и количественно измеряемый морфологический процесс; целесообразна стандартизация морфометрической и иммуногистохимической оценки.

Ключевые слова: отравление угарным газом; лёгкие; альвеолярное повреждение; отёк лёгких; эмфизема; морфометрия; CD68; каспаза-3; иммуногистохимия; судебная медицина.

Introduction

1.1. The global burden of carbon monoxide poisoning

Carbon monoxide (CO) is a colourless, odourless, tasteless and non-irritating gas generated by the incomplete combustion of carbon-containing fuels, and it remains the leading cause of fatal poisoning in many countries [7, 9, 11]. Because it gives the victim no sensory warning, exposed persons commonly remain in a contaminated atmosphere until consciousness is lost — the reason for its traditional designation as the “silent killer” [12].

The most authoritative contemporary estimate of its burden derives from the Global Burden of Disease (GBD) programme. In 2021 the global mortality rate attributable to unintentional CO poisoning was 0.366 per 100 000 population (95% uncertainty interval 0.276–0.415), corresponding to 28 900 deaths and 1.18 million years of life lost; nearly 70% of deaths occurred in men, the largest absolute number of deaths fell in the 50–54-year age band, and the highest age-specific rate — 1.96 per 100 000 — was recorded in persons aged 85 years and over [1]. Regional inequality is pronounced: eastern Europe carried the highest age-standardised mortality at 2.12 per 100 000 [1]. Within Asia the heaviest burden in 2021 was borne by Mongolia (2.60 per 100 000), Afghanistan (1.76) and Kazakhstan (1.70) [3]. These differences are summarised in Figure 1.

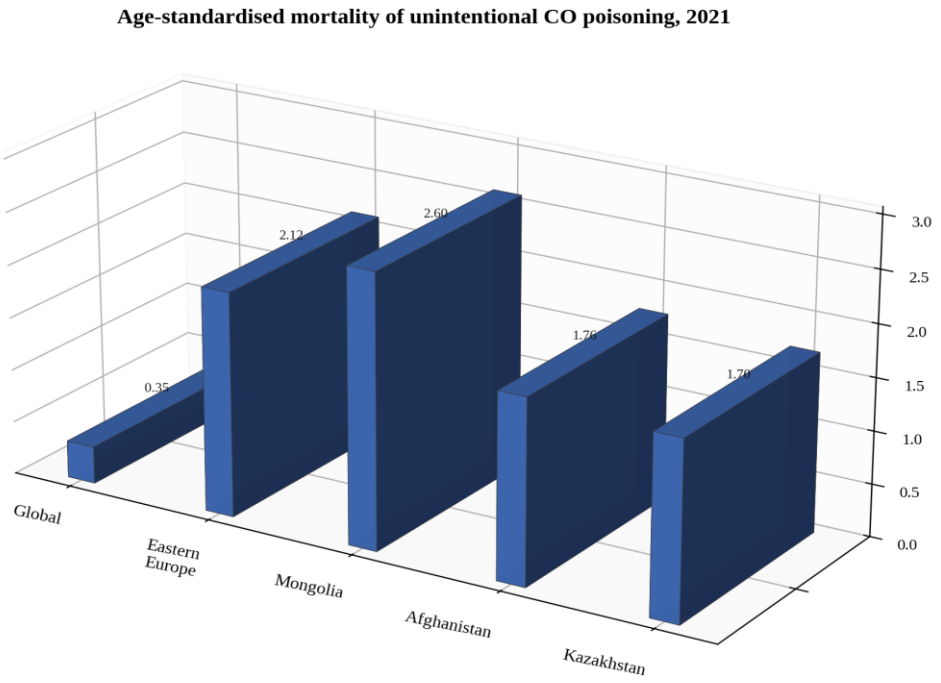

Figure 1. Age-standardised mortality due to unintentional carbon monoxide poisoning in selected regions and countries, 2021 (deaths per 100 000 population). Data from [1, 3]. The editable data series is provided in sheet “Fig1” of the accompanying workbook.

Both incidence and mortality have fallen substantially over three decades. The age-standardised incidence declined by approximately 35% between 1990 and 2021 (from 12.13 to 7.87 per 100 000) and mortality by approximately 54% (from 0.76 to 0.35 per 100 000) [2]; the GBD collaborators independently documented a 53.5% fall in the age-standardised mortality rate between 2000 and 2021 [1]. The decline, however, has been geographically uneven, and in absolute terms roughly 294 000 acute poisonings still occur worldwide each year [2]. Figure 2 illustrates this trend. In Central Asia, where solid-fuel and gas heating remain widespread and domestic ventilation is frequently inadequate, the winter clustering of poisonings keeps CO among the leading toxicological emergencies; comparable seasonal patterns have been documented in Turkey and in the WHO European Region [5, 6].

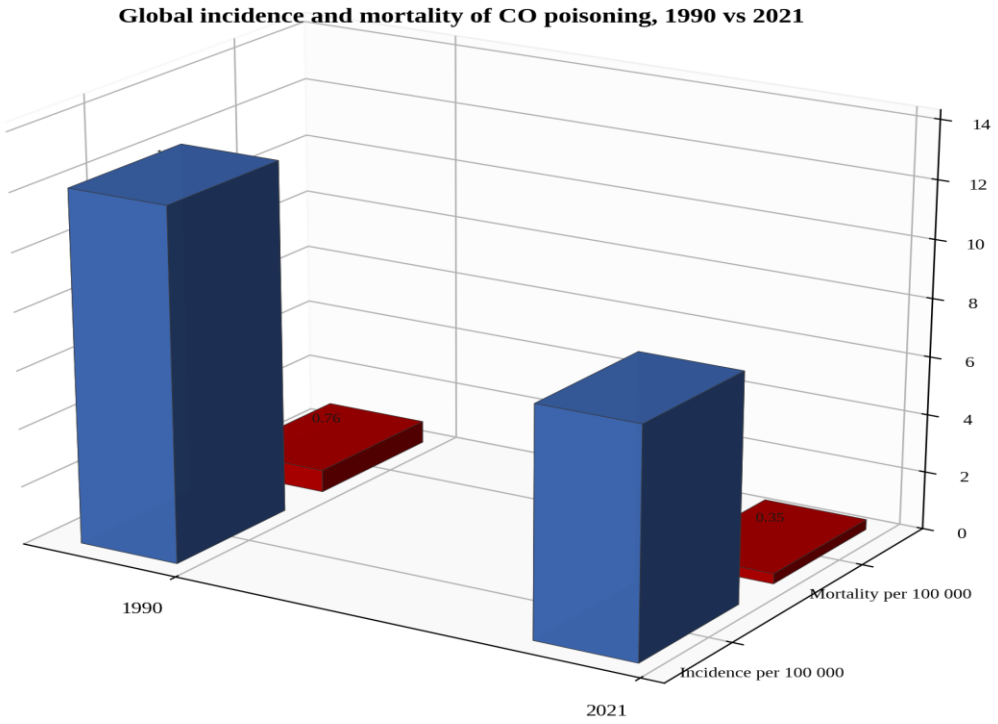

Figure 2. Global age-standardised incidence and mortality of carbon monoxide poisoning, 1990 versus 2021 (rates per 100 000 population). Data from [2].

Two features of this epidemiology bear directly on the present review. First, the majority of deaths occur in middle-aged and elderly persons, in whom cardiopulmonary reserve and reparative capacity are already reduced; the morphological response of the lung is therefore unlikely to be age-independent. Second, an increasing proportion of exposed individuals now survive the acute episode, which shifts clinical and pathological attention from immediate lethality towards delayed and residual organ damage.

1.2. The lung as portal of entry and as target organ

CO exerts toxicity only when inhaled. It crosses the alveolar–capillary membrane by simple diffusion and binds the ferrous iron of haem with an affinity 200–250 times greater than that of oxygen, generating carboxyhaemoglobin (COHb) [8, 10, 11]. The consequences are threefold: the oxygen-carrying capacity of blood falls; the oxyhaemoglobin dissociation curve is displaced to the left and becomes more hyperbolic, so that the oxygen still bound is released to the tissues less readily; and CO binds additional haemoproteins — myoglobin, mitochondrial cytochrome c oxidase, catalase, peroxidase and neuroglobin — thereby impairing cellular respiration directly [8, 10, 13, 14].

Tissue injury is therefore not purely hypoxic. Reoxygenation generates reactive oxygen and nitrogen species; CO displaces nitric oxide from haem proteins, and the resulting free nitric oxide reacts with superoxide to form peroxynitrite. Lipid peroxidation, xanthine dehydrogenase-to-oxidase conversion, platelet–neutrophil interaction with neutrophil degranulation and myeloperoxidase release amplify a sterile inflammatory response, and an adduct-driven, immune-mediated component prolongs injury well beyond the elimination of the gas itself [16, 17, 18, 28, 29].

Because the brain and the myocardium have the highest metabolic rates, they have traditionally dominated both the clinical literature and the classical description of CO pathology [8, 9, 30]. The lung, however, occupies a unique position: it is at once the route of entry, the organ of elimination and a tissue exposed to the highest partial pressure of the toxicant. Experimental work has shown for more than half a century that CO alters alveolar epithelial permeability and lung ultrastructure independently of systemic hypoxaemia. Fein and colleagues demonstrated a measurable increase in alveolar epithelial permeability after CO exposure [31]; the classical ultrastructural study of Niden and

Schulz described swelling of alveolar epithelial and capillary endothelial cells, mitochondrial and nucleoplasmic swelling, denudation of capillary basement membranes and capillary platelet thrombosis, and — crucially — reported that the inhaled CO concentration predicted these changes better than either blood COHb level or exposure duration, implying a direct pulmonary effect [20]. Fisher and co-workers similarly documented functional and structural pulmonary consequences of CO exposure [19].

1.3. Why the morphology of the lung deserves separate attention

Three considerations justify a dedicated morphological synthesis. The first is forensic. Pulmonary findings are among the most consistent features at autopsy: in a series of 127 fatal CO poisonings, Pehlivan et al. recorded pulmonary oedema in 80%, emphysematous change in 42%, haemorrhage in 27% and congestion in 13% of cases [25]; Finck's classical review of 567 autopsies reported congestion and/or oedema in 66% and haemorrhage in 7% [27]. Critically, Pehlivan et al. found no statistically significant correlation between blood COHb concentration and the degree of pulmonary oedema ($p = 0.434$), haemorrhage ($p = 0.307$), congestion ($p = 0.227$) or emphysematous change ($p = 0.944$), which demonstrates that the morphological picture cannot be inferred from the biochemical marker and must be assessed in its own right [25].

The second consideration is clinical. Radiographic abnormalities — ground-glass opacity, perihilar haze, peribronchial and perivascular cuffing, and frank intra-alveolar oedema — are demonstrable in roughly one third of patients with severe acute poisoning [23, 24], and severe cases may progress to acute respiratory failure and acute respiratory distress syndrome requiring mechanical ventilation or extracorporeal support [32, 33]. A nationwide population-based cohort study from the Republic of Korea has further shown that survivors of CO poisoning carry an increased subsequent risk of chronic lung disease, indicating that the pulmonary consequences are not confined to the acute episode [22].

The third consideration is experimental. Lee and colleagues exposed rats to 1500 ppm CO for three hours and, six weeks later, demonstrated emphysematous change with a significantly increased mean linear intercept ($p = 0.0007$), together with altered inflammatory signalling in lung homogenates and raised serum Krebs von den Lungen-6 (KL-6) — the first direct evidence that a single acute exposure produces durable structural remodelling of the alveolar compartment [21]. This finding reframes CO lung injury as a process with a long tail rather than a transient event.

1.4. Aim of the review

The present narrative review synthesises the evidence published mainly over the last decade on the macroscopic, microscopic, morphometric, histochemical and immunohistochemical features of the lung after acute CO poisoning. It organises these findings into a staged morphogenetic model, examines the modifying influence of age, and defines the assessment framework required for diagnostic, forensic and experimental practice.

2. Materials and methods

This work is a narrative (non-systematic) review. Electronic searches were performed in PubMed/MEDLINE, Scopus, Web of Science, Google Scholar and eLIBRARY using combinations of the terms "carbon monoxide poisoning", "carboxyhaemoglobin", "lung injury", "pulmonary oedema", "alveolar damage", "emphysema", "morphometry", "alveolar septal thickness", "mean linear intercept", "glycosaminoglycans", "alcian blue", "CD68", "caspase-3", "apoptosis", "immunohistochemistry", "forensic autopsy", "hyperbaric oxygen" and "DLCO". Priority was given to peer-reviewed articles published between 2015 and 2026, supplemented by earlier seminal studies that established key concepts and remain the primary source of ultrastructural and permeability data. Both clinical material (patient cohorts, radiological series, forensic autopsy series) and experimental material (rodent and large-animal inhalational models) were included, together with relevant systematic reviews, mechanistic reviews and clinical guidance documents. Case reports without morphological documentation and non-peer-reviewed material were excluded.

Extracted data were organised along three axes — level of biological organisation (organ, tissue, cell, molecule), time after exposure (early, up to 24 h; delayed, from 24 h to 6 weeks), and setting (human clinical, human post-mortem, experimental) — and are presented descriptively. Quantitative pooling was not attempted, because heterogeneity of species, exposure protocol, severity and

observation time points precluded meaningful meta-analysis. Fifty sources were retained for synthesis. The quantitative values used to construct Figures 1–3 and 6 and Tables 2–6 were taken directly from the cited primary studies; Figures 4 and 5 present the authors' own preliminary experimental data obtained in outbred white rats and are explicitly identified as such. All figures are supplied as an editable Microsoft Excel workbook (three-dimensional charts, Times New Roman) accompanying this article.

Table 1.

Streams of evidence analysed in this review

Evidence stream	Typical setting / model	Principal read-outs	Representative sources
Epidemiological syntheses	GBD 2021, national registries	Mortality, incidence, DALYs, age and sex distribution	[1–6]
Mechanistic reviews	Human and animal, in vitro	COHb kinetics, mitochondrial inhibition, oxidative stress, immune activation	[8, 10, 13–18, 28, 29]
Clinical and radiological cohorts	Emergency departments, hyperbaric centres	Chest radiograph and CT patterns, respiratory failure, ventilation, outcome	[22–24, 32–35]
Forensic autopsy series	Fatal poisonings (n = 127 and n = 567)	Macroscopic and microscopic lung pathology, correlation with COHb	[25, 27, 36, 37]
Experimental inhalational models	Rat, mouse, sheep	Histology, ultrastructure, mean linear intercept, permeability, biomarkers	[19–21, 26, 31, 38]
Morphometric and histochemical studies	Rodent lung, human post-mortem	Alveolar septal thickness, airspace area, bronchiolar and arteriolar dimensions, glycosaminoglycans	[21, 39–41]
Immunohistochemical studies	Acute lung injury of varied aetiology	CD68, CD163, caspase-3, TUNEL, pyroptosis markers	[42–45]
Diagnostic technology	CO-oximetry, ABG, imaging, DLCO, artificial intelligence	Accuracy, sensitivity, specificity, AUC	[46–50]

3. Results of the Literature Synthesis

3.1. Mechanistic basis of carbon monoxide-induced pulmonary injury

The mechanisms operating in the lung can be grouped into five interlocking axes, summarised in Table 2. The haemic axis — COHb formation with leftward displacement of the dissociation curve — produces systemic tissue hypoxia and is the classical explanation of CO toxicity [8, 10]. The mitochondrial axis reflects the binding of CO to the haem a3 moiety of cytochrome c oxidase, which blocks electron transfer, reduces ATP synthesis and increases electron leak; Zhang and Piantadosi demonstrated that this generates measurable mitochondrial oxidative stress in vivo [16]. The oxidative axis comprises reactive oxygen species production, lipid peroxidation and peroxynitrite formation, processes analysed in depth by Akyol and colleagues [28]. The inflammatory axis involves platelet–neutrophil aggregation, neutrophil degranulation, myeloperoxidase release, macrophage activation and cytokine production; Thom and co-workers showed that the delayed component of CO pathology is immune-mediated and adduct-driven rather than simply hypoxic [17]. The apoptotic axis reflects mitochondrial permeability transition, cytochrome c release and caspase activation, demonstrated after CO poisoning by Piantadosi et al. [18].

It is essential to note the biological duality of CO. At low, physiological or pharmacological concentrations, CO produced endogenously by haem oxygenase acts as a gasotransmitter with vasoregulatory, anti-inflammatory and anti-apoptotic properties, and inhaled low-dose CO is protective in several models of experimental lung injury — hyperoxic, endotoxin-induced and ventilator-induced [13, 14, 15, 38, 51]. The morphology described in the remainder of this review is that of high-concentration acute intoxication, in which these regulatory actions are overwhelmed. This dose-dependence explains why the same molecule appears both as a therapeutic candidate and as the commonest lethal poison, and it warns against extrapolating from low-dose protective models to acute poisoning.

Table 2.

Principal mechanisms of carbon monoxide toxicity relevant to the lung

Mechanistic axis	Molecular target / trigger	Pulmonary morphological correlate	Sources
Haemic hypoxia	Haemoglobin (COHb), leftward shift of the dissociation curve	Congestion, generalised hypoxic injury of alveolar epithelium and endothelium	[8, 10, 11]
Mitochondrial inhibition	Cytochrome c oxidase (haem a3), myoglobin, catalase	Alveolocyte and endothelial mitochondrial swelling, hydropic and vacuolar dystrophy, ATP depletion	[13, 16, 20, 30]
Oxidative and nitrosative stress	ROS, lipid peroxidation, NO displacement, peroxynitrite	Membrane damage of the air–blood barrier, increased alveolar–capillary permeability, oedema	[17, 28, 31]
Inflammatory activation	Platelet–neutrophil interaction, myeloperoxidase, macrophage cytokines	Neutrophil and macrophage infiltration, interstitial and intra-alveolar exudate, CD68 up-regulation	[17, 21, 42, 43]
Apoptosis and regulated cell death	Cytochrome c release, caspase-9/caspase-3, pyroptotic cascades	Loss of type I and type II alveolocytes, denuded basement membrane, caspase-3 up-regulation	[18, 44, 45]
Matrix and repair dysregulation	Protease–antiprotease imbalance, TGF-β, KL-6	Emphysematous alveolar destruction, septal thickening, focal fibrosis	[21, 39, 40]

3.2. Clinical and radiological pulmonary phenotypes

Clinically, the respiratory system is affected far more often than the classical literature implies. The two commonest overt manifestations are pulmonary oedema and pneumonia [25, 32]. In severe poisoning, airway obstruction, atelectasis and pulmonary oedema together may precipitate acute respiratory failure requiring intubation and mechanical ventilation, and the need for endotracheal intubation is strongly associated with mortality [33, 34].

Table 3. Clinical and radiological pulmonary phenotypes of acute carbon monoxide poisoning

Phenotype	Timing	Principal features	Reported frequency / comment
Subclinical interstitial oedema	0–24 h	Ground-glass density, perihilar haze, perivascular cuffing; hypoxaemia	Radiographic abnormality in 29–36% of severe cases [23]
Overt pulmonary oedema	0–48 h	Intra-alveolar oedema, frothy serous or sero-haemorrhagic fluid, dyspnoea	Clinically manifest in ~6.6% of severe cases; commonest autopsy finding (80%) [23, 25]
Acute respiratory failure / ARDS	Hours–days	Airway obstruction, atelectasis, diffuse alveolar damage, refractory hypoxaemia	Requires mechanical ventilation; intubation strongly linked to mortality [33–35]
Combined inhalational injury (fire)	Immediate	Airway erythema and oedema, carbonaceous deposits, pseudomembranous casts, cytokine storm	High mortality; may require ECMO [32, 35]
Secondary pneumonia / bronchitis	Days	Bronchial drainage failure, mucus plugging, bacterial superinfection	Pneumonia 3% and bronchitis 5% at autopsy; negatively correlated with COHb [25]
Delayed pneumonitis	Days–weeks	New cardiorespiratory symptoms after apparent recovery; inflammatory infiltration	Documented in case series; pathogenesis undetermined [24]
Residual structural change	Weeks–years	Emphysematous alveolar enlargement, reduced diffusion capacity, chronic lung disease	Increased risk of lung disease in nationwide cohort; emphysema at 6 weeks in rats [21, 22]

When exposure occurs in the context of a fire, the CO component is compounded by thermal and chemical inhalational injury — mucosal erythema and oedema, carbonaceous deposits, pseudomembranous casts — and by the simultaneous inhalation of cyanide, hydrogen chloride, aldehydes and nitrogen and sulphur oxides; in such patient's acute respiratory distress syndrome and cytokine storm may follow [32, 35].

Radiologically, the earliest and commonest abnormality is a diffuse, homogeneous ground-glass density, followed by perihilar haze with peribronchial and perivascular cuffing and, in more advanced cases, frank intra-alveolar oedema; patients presenting with ground-glass density show marked hypoxaemia on admission [23]. In a classical series of 62 patients, 18 (29%) had an abnormal chest radiograph [23], and in a further series of 61 patients with severe poisoning 22 (36.1%) had radiographic abnormality although only four (6.6%) had clinically overt pulmonary oedema — a discrepancy indicating that subclinical pulmonary involvement is considerably more frequent than the bedside picture suggests. Delayed pulmonary presentations, including inhalational pneumonitis appearing after apparently uneventful recovery, have also been documented, paralleling the better-known delayed neuropsychiatric sequelae [24, 32]. Table 3 summarises these phenotypes.

3.3. Macroscopic morphology of the lung

At autopsy the lungs of a person dying of acute CO poisoning are typically increased in volume and weight and firmer than normal, with reduced elasticity and a moist cut surface reflecting severe pulmonary oedema. Venous congestion combined with the presence of carboxyhaemoglobin gives the parenchyma a characteristic bright cherry-red or deep red hue, although this classical colour is by no means invariable and is absent in a substantial minority of cases. Subpleural petechial haemorrhages, produced by capillary wall damage and increased vascular permeability, are frequent; frothy serous or sero-haemorrhagic fluid exudes from the cut surface, confirming alveolar oedema and disruption of the alveolar–capillary barrier. In severe cases diffuse congestion may be accompanied by focal atelectasis in some lobes and, conversely, by compensatory emphysematous distension in others [25, 27, 36, 37].

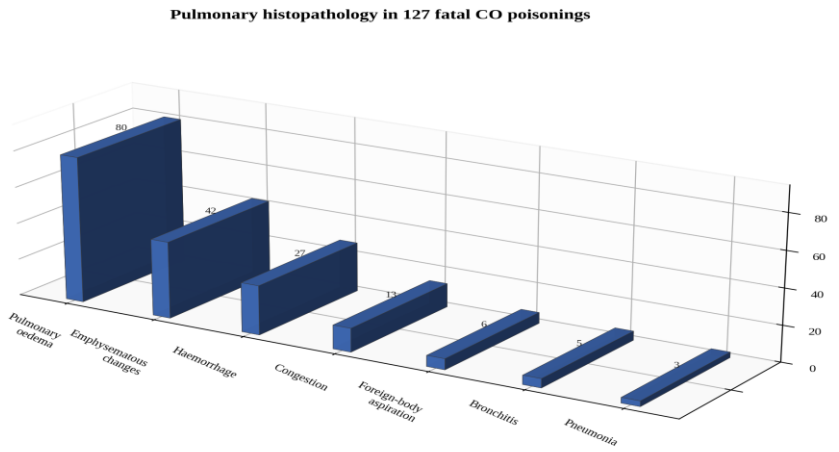

Figure 3. Frequency of pulmonary histopathological findings in 127 fatal carbon monoxide poisonings (forensic autopsy series). Data from [25]. For comparison, Finck reported congestion and/or oedema in 66% and haemorrhage in 7% of 567 autopsies [27].

The quantitative distribution of these findings in the largest recent forensic series is shown in Figure 3. Pulmonary oedema dominated (80%), followed by emphysematous change (42%), haemorrhage (27%) and congestion (13%); foreign-body aspiration, bronchitis and pneumonia were less frequent [25]. Two correlations reported in that series deserve emphasis. First, a negative correlation was found between COHb concentration and both pneumonia ($p = 0.027$) and bronchitis (p

= 0.006), consistent with the interpretation that patients who survive long enough to develop infective complications have, by definition, cleared much of their COHb. Second, a negative correlation was observed between oedema and emphysematous change ($p = 0.018$) and between congestion and emphysematous change ($p < 0.001$), which suggests that the exudative and the destructive–emphysematous patterns are, to some degree, alternative or sequential rather than concurrent expressions of injury [25]. This observation is one of the empirical foundations of the two-phase model advanced in Section 4.2.

3.4. Microscopic morphology: the early vascular–exudative phase

Light-microscopic studies of the first hours after exposure describe a consistent constellation dominated by microcirculatory disturbance. Alveolar capillaries and venules are sharply dilated, engorged and bulge into the alveolar lumen; erythrocytes are deformed and aggregated, and micro-thrombi form preferentially in the wall-adjacent portion of venules in accordance with the distribution of flow velocity. Bronchial arterial vessels are in spasm. Leucocyte counts within the vessels rise. These changes confirm that a hydrostatic factor operates early in the genesis of oedema, alongside the permeability factor [26, 36].

Interalveolar septa become oedematous and uniformly thickened; plasma components exude into the interstitium and then into the alveolar spaces, where a homogeneous, eosinophilic, protein-rich transudate accumulates. Diapedetic haemorrhage appears in interalveolar septa and in perivascular zones, and in more severe cases intra-alveolar and stromal haemorrhages are distributed diffusely throughout the parenchyma. Bronchioles are deformed and spastic; the ciliated epithelium shows vacuolar dystrophy, cytoplasmic swelling, nuclear pyknosis and focal desquamation, and mucous plugs containing shed epithelial cells obstruct the lumen. Foci of atelectasis and partial alveolar collapse alternate with zones of acute local emphysema in which alveolar ducts and alveoli are sharply distended and the interalveolar septa markedly attenuated. Reactive mononuclear infiltration, features of desquamative alveolitis and diffuse small-focal dystelectasis complete the picture [20, 26, 36, 37].

At the ultrastructural level, this phase corresponds to swelling of alveolar epithelial cell mitochondria and nucleoplasm, swelling of capillary endothelium and alveolar epithelium sufficient to narrow both capillary and alveolar lumina into slit-like spaces, formation of defects in the alveolar lining with denudation of the capillary basement membrane, and capillary platelet thrombosis [20]. Functionally, these changes are expressed as a measurable increase in alveolar epithelial permeability [31], falling arterial oxygen tension, impaired carbon dioxide exchange and combined metabolic and respiratory acidosis. Damage to type II alveolocytes reduces surfactant synthesis, predisposing the alveoli to collapse and creating the substrate for micro-atelectasis and worsening ventilation–perfusion mismatch.

3.5. Microscopic morphology: the delayed inflammatory–destructive phase

In animals and patients surviving beyond the first day, the morphological emphasis shifts. Exudation recedes; macrophage and lymphocyte infiltration of the interstitium becomes prominent; and the destructive and reparative processes that determine the long-term outcome begin. Interalveolar septa that were uniformly oedematous in the early phase now become irregularly thickened, focally homogenised and, in places, discontinuous. Adjacent alveolar spaces coalesce through these septal breaks to form enlarged airspaces containing sero-haemorrhagic fluid, macrophages and cellular debris. Bronchiolar epithelial desquamation becomes diffuse rather than focal, and peribronchial infiltration and bronchiolar wall thickening appear [21, 36, 37].

The most important recent contribution to this phase is the demonstration by Lee and colleagues that a single three-hour exposure to 1500 ppm CO produces, six weeks later, emphysematous change with a significantly increased mean linear intercept ($p = 0.0007$), accompanied by changes in inflammatory signalling molecules in lung homogenates and by elevation of the alveolar epithelial damage marker KL-6 [21]. The authors interpreted this as mechanistically analogous to smoking-related emphysema, in which oxidative stress disturbs the neutrophil elastase–antielastase balance and permits proteolytic destruction of the alveolar wall. Two features distinguish the CO model, however. First, exposure is a single high-concentration event rather than a chronic low-dose one. Second, the emphysema develops in the absence of the particulate burden that accompanies tobacco smoke, which isolates the gaseous and hypoxic–oxidative components of the injury. Together with the nationwide

cohort evidence of increased subsequent lung disease among survivors [22], this establishes that the structural consequences of a single acute poisoning are durable.

Where exposure is repeated or the reparative response is inadequate, interstitial fibroblast proliferation and collagen synthesis increase and focal interstitial fibrosis develops, thickening the interalveolar septa, reducing pulmonary elasticity and diffusing capacity, and providing the morphological substrate for chronic respiratory insufficiency [21, 39, 40].

3.6. Quantitative morphometry of the lung

Morphometry converts the descriptive categories above into reproducible numbers, and it is the element most conspicuously missing from the published CO literature. The parameters that have proved informative in experimental toxic and hypoxic lung injury are the alveolar septal (alveolar wall) thickness, the alveolar airspace area, the mean linear intercept, the bronchiolar diameter and wall thickness, and the arteriolar diameter and wall thickness. Of these, only the mean linear intercept has been formally reported after CO poisoning, and only at a single late time point [21].

Figure 4 and Table 4 present the authors' own preliminary morphometric data in outbred white rats, included here to illustrate the informational yield of the approach rather than as validated reference values. Alveolar septal thickness rose from 10.42 µm in 3-month-old controls to 12.42 µm at 6 h (+19.2%) and fell to 11.21 µm at 7 days, remaining 7.6% above control. In 9-month-old animals the corresponding values were 13.48 µm, 16.25 µm (+20.5%) and 14.67 µm (+8.8% above control). The alveolar airspace area moved reciprocally, falling by 5.3% and 4.6% respectively at 6 h and recovering only partially by day 7. Bronchiolar and arteriolar wall thickness increased by 13.9–16.6% in the young animals and by 13.8–14.6% in the older animals at 6 h, again with incomplete normalisation by day 7.

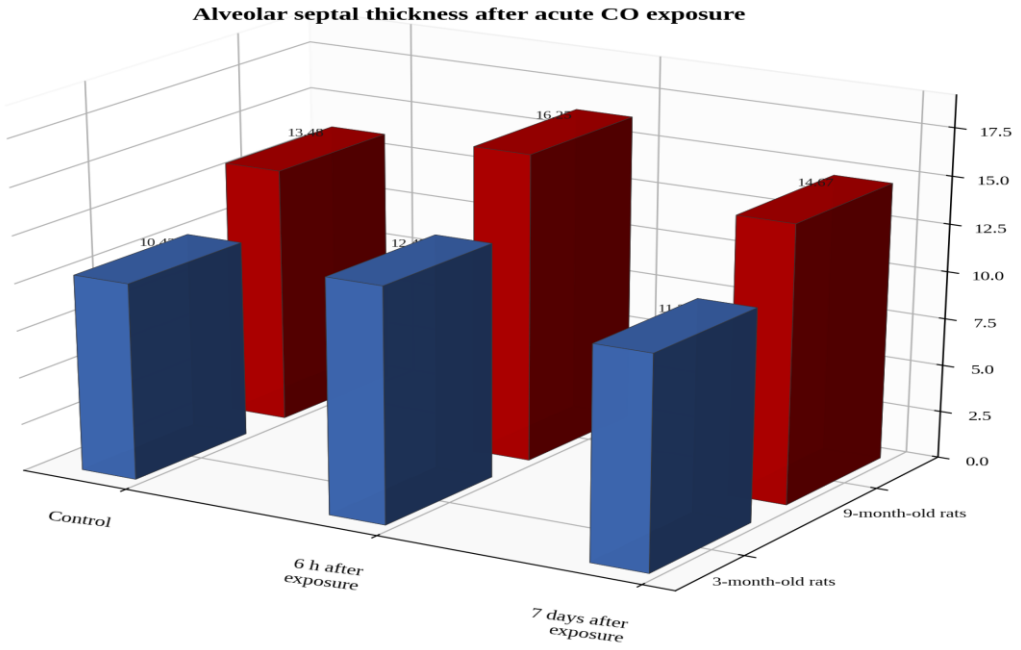

Figure 4. Alveolar septal thickness (µm) in 3- and 9-month-old outbred white rats before and after acute carbon monoxide exposure. Authors' own preliminary experimental data; haematoxylin–eosin, light microscopy, morphometry with NLCD-307B.

Table 4. Representative morphometric indices of the lung after acute carbon monoxide exposure (authors' own preliminary experimental data)

Index	3 months: control / 6 h / 7 days	9 months: control / 6 h / 7 days	Direction and magnitude
Alveolar septal thickness (μm)	10.42 / 12.42 / 11.21	13.48 / 16.25 / 14.67	↑ 19.2% and 20.5% at 6 h; incomplete recovery at day 7
Alveolar airspace area (μm²)	3786.76 / 3587.84 / 3714.81	3592.15 / 3426.45 / 3481.62	↓ 5.3% and 4.6% at 6 h; partial recovery
Bronchiolar diameter (μm)	225.46 / 239.36 / 231.16	241.51 / 254.22 / 247.14	↑ 6.2% and 5.3% at 6 h
Bronchiolar wall thickness (μm)	27.84 / 31.72 / 29.61	30.00 / 36.29 / 35.22	↑ 13.9% and 14.6% at 6 h; 11.2% still elevated at day 7 in older animals
Arteriolar diameter (μm)	61.75 / 64.85 / 62.19	65.12 / 69.81 / 67.21	↑ 5.0% and 7.2% at 6 h
Arteriolar wall thickness (μm)	11.45 / 13.35 / 12.13	12.56 / 14.29 / 13.28	↑ 16.6% and 13.8% at 6 h

Three points follow. First, the maximum of every index occurs early, at 6 h, which identifies the vascular–exudative phase as the period of greatest quantitative deviation. Second, none of the indices returns fully to control by day 7, confirming that structural change outlasts the exudative episode. Third, the deviation is consistently larger and the recovery consistently slower in the older animals — a point developed in Section 3.9.

3.7. Histochemistry of the extracellular matrix

Alcian blue staining at pH 2.5 detects acidic mucopolysaccharides and glycosaminoglycans and offers a sensitive, inexpensive means of tracking two distinct processes in the injured lung: the hydration of the interstitial matrix that accompanies oedema, and the synthesis of new matrix that accompanies repair. In the early phase, diffuse, moderate alcian-blue positivity appears in the interalveolar septa and perivascular stroma, reflecting the accumulation of oedema fluid and increased stromal hydration; the diffuse, non-focal distribution indicates that the process is exudative rather than destructive. In the delayed phase the pattern diverges according to the outcome of repair. Where reparative regeneration predominates, bright focal positivity appears in newly forming connective tissue and regenerating alveolar walls, indicating active synthesis of glycosaminoglycan-rich matrix. Where destruction and sclerosis predominate, the reaction becomes weak, uneven and focal, indicating that matrix turnover has been diverted from physiological regeneration towards sclerotic reorganisation [39–41].

This distinction has practical value: an alcian-blue reaction that is diffuse and moderate is a marker of the exudative phase, one that is bright and focal is a marker of productive repair, and one that is weak and patchy is a marker of failing repair. Because the extracellular matrix is also the substrate on which the protease–antiprotease imbalance implicated in CO-related emphysema acts [21], histochemical assessment of matrix links the exudative and the destructive components of the injury.

3.8. Immunohistochemistry: CD68 and caspase-3

Two markers capture the two dominant cellular processes. CD68 is a lysosomal glycoprotein of the monocyte–macrophage lineage; its expression quantifies both the resident alveolar macrophage population and the macrophages recruited and activated during inflammation. Caspase-3 is the principal effector caspase of the apoptotic cascade; its expression quantifies programmed cell death in alveolar epithelium, endothelium and interstitial cells.

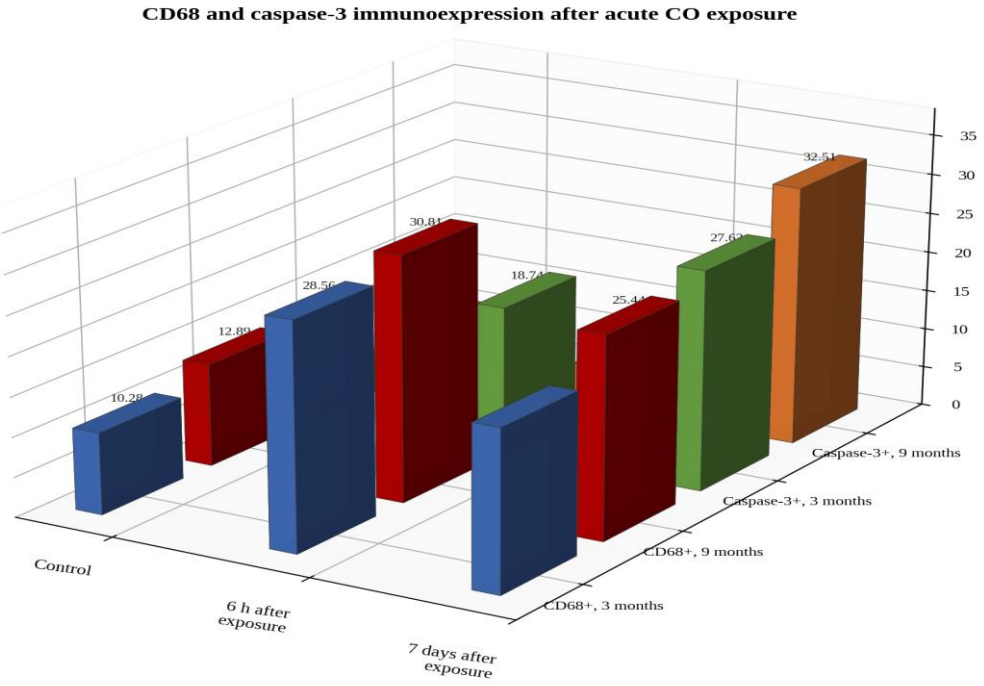

Figure 5. CD68 and caspase-3 immunoexpression (percentage of positive cells) in lung tissue of 3- and 9-month-old outbred white rats before and after acute carbon monoxide exposure. DAB chromogen, quantification with QuPath 0.7.0 in five fields at ×200–×400. Authors' own preliminary experimental data.

Their combined assessment therefore separates the inflammatory from the cell-death component of injury, which conventional staining cannot do. This paired approach has been validated in acute lung injury of other aetiologies: in fatal COVID-19, activation of CD68+/CD163+ macrophages and caspase-3 expression tracked the severity of diffuse alveolar damage and the progression to organising pneumonia and fibrosis [42]; in hyperoxic neonatal lung injury, CD68 immunohistochemistry quantified macrophage involvement in impaired alveolarisation [43]; and caspase-3 immunoexpression in airway epithelium rose from 15.86 ± 1.84 in controls to 41.62 ± 3.46 at 24 h and 55.24 ± 6.80 at 72 h of hyperoxia, establishing the time course of apoptosis in oxidative lung injury [44]. Comparable data for CO poisoning have not previously been published.

Figure 5 and Table 5 present the authors' own preliminary immunohistochemical findings. In 3-month-old animals, CD68 expression rose from a baseline of 10.28% to 28.56% at 6 h (a 2.78-fold increase) and declined to 20.25% at 7 days, whereas caspase-3 rose from 4.66% to 18.74% at 6 h (a 4.02-fold increase) and continued to rise to 27.63% at 7 days. In 9-month-old animals, CD68 rose from 12.89% to 30.81% at 6 h (2.39-fold) and remained elevated at 25.44% on day 7, whereas caspase-3 was essentially unchanged at 6 h (5.59% to 5.37%) before rising steeply to 32.51% by day 7. In both age groups caspase-3 exceeded CD68 at day 7, by 7.38 and 7.07 percentage points respectively.

3.9. Age as a modifier of the pulmonary response

Age emerges from every level of the evidence as a decisive modifier. Epidemiologically, mortality rises steeply with age, reaching 1.96 per 100 000 in persons of 85 years and over, and the largest absolute number of deaths falls in the 50–54-year band [1]. Clinically, older patients present with deeper impairment of consciousness, more rapid development of respiratory insufficiency and a higher frequency of secondary pneumonia and late cardiopulmonary failure, in part because coexisting cardiovascular disease limits compensation. Morphologically, the same divergence is visible: in young animals the changes are predominantly reactive and functional — serous oedema, capillary hyperaemia, focal epithelial desquamation, brisk macrophage and lymphocyte response, with the general architecture preserved — whereas in older animals they are diffuse and destructive, with septal

homogenisation and rupture, coalescence of airspaces, sero-haemorrhagic exudate, venular thrombosis and marked peribronchial and perivascular oedema, accompanied by a comparatively muted cellular reaction.

Table 5. Immunohistochemical markers applicable to carbon monoxide-induced lung injury

Marker	Biological meaning	Reported behaviour after acute injury	Interpretation
CD68	Lysosomal glycoprotein of monocytes and macrophages; resident and recruited macrophages	Rises 2.4–2.8-fold within 6 h and remains elevated at day 7; peaks earlier than caspase-3	Marker of the inflammatory–phagocytic component; early peak identifies the acute reactive phase [42, 43]
Caspase-3	Principal effector caspase of apoptosis	Rises early in young animals but late in older ones; highest values at day 7 in both	Marker of the cell-death component; late dominance indicates continuing structural damage [18, 44]
CD163	Marker of the alternatively activated (M2) macrophage	Co-expressed with CD68 in organising pneumonia and fibrosis	Distinguishes reparative from pro-inflammatory macrophage polarisation [42]
TUNEL	DNA fragmentation in situ	Correlates with cleaved caspase-3 in epithelial apoptosis	Independent confirmation of apoptosis; complements caspase-3 [44, 45]
KL-6	Glycoprotein released by damaged type II alveolocytes	Elevated after experimental CO poisoning and in fibro-emphysematous disease	Serum correlate of alveolar epithelial injury; links morphology to a blood test [21]

The immunohistochemical data quantify this divergence in an instructive way. In young animals inflammation and apoptosis were activated in parallel from the outset. In older animals the early response was almost purely macrophagic, with caspase-3 unchanged at 6 h, and apoptosis was deferred to the later period, when it rose to the highest values recorded in the study. This temporal dissociation suggests that ageing does not simply amplify the injury but reorders it, delaying the apoptotic clearance of damaged cells and thereby prolonging the window during which inflammation and structural disorganisation coexist. It is consistent with the slower and less complete morphometric normalisation observed in the same animals and with the weak, patchy alcian-blue reaction indicating failing matrix repair.

3.10. Diagnostic technologies relevant to pulmonary complications

Diagnosis proceeds on two fronts: confirming the poisoning and characterising the pulmonary consequences. For the first, co-oximetry combined with arterial blood gas analysis remains the reference standard for measuring COHb, whereas conventional pulse oximetry is unreliable because it cannot distinguish carboxyhaemoglobin from oxyhaemoglobin and may therefore display falsely normal saturation despite profound tissue hypoxia [46, 47]. Non-invasive pulse CO-oximeters offer speed but lose accuracy with reduced peripheral perfusion or motion artefact, and current emergency medicine guidance advises against relying on them for diagnosis [34, 46]. Serum lactate has been proposed as an adjunctive severity marker, and prognostic scoring systems combining clinical and laboratory variables have been developed [35, 47]. It must be emphasised that COHb concentration predicts neither clinical severity nor — as Section 3.3 showed — the pulmonary morphological picture [25].

Regarding therapy, the evidence base for hyperbaric oxygen remains contested. A network meta-analysis of eight randomised trials (n = 1785) found no advantage of hyperbaric over normobaric oxygen and signalled possible harm from repeated sessions [48], and a 2026 systematic review and meta-analysis, including a subgroup analysis restricted to pressures of 2.5 atmospheres absolute or above, likewise found no significant benefit for mortality or neurological outcome, rating the quality of evidence as low to very low [49]. Current professional guidance therefore positions hyperbaric oxygen as a therapeutic option in selected patients rather than a mandated treatment [34]. Rarely, pulmonary oedema has been reported as a complication of hyperbaric therapy itself, which is a further argument for careful pulmonary assessment before and after treatment.

For characterising the lung, chest radiography and computed tomography define the pattern and extent of oedema, consolidation and atelectasis, and the diffusing capacity of the lung for carbon monoxide (DLCO) provides the functional counterpart of the alveolar–capillary morphology described in this review; DLCO falls when the gas-exchange surface is destroyed, as in emphysema, or when the alveolar–capillary membrane is diffusely damaged [50]. Its use in survivors of CO poisoning would provide a direct functional test of the emphysematous remodelling demonstrated experimentally [21], although the measurement itself uses carbon monoxide as the test gas and must be interpreted with care when residual COHb is present.

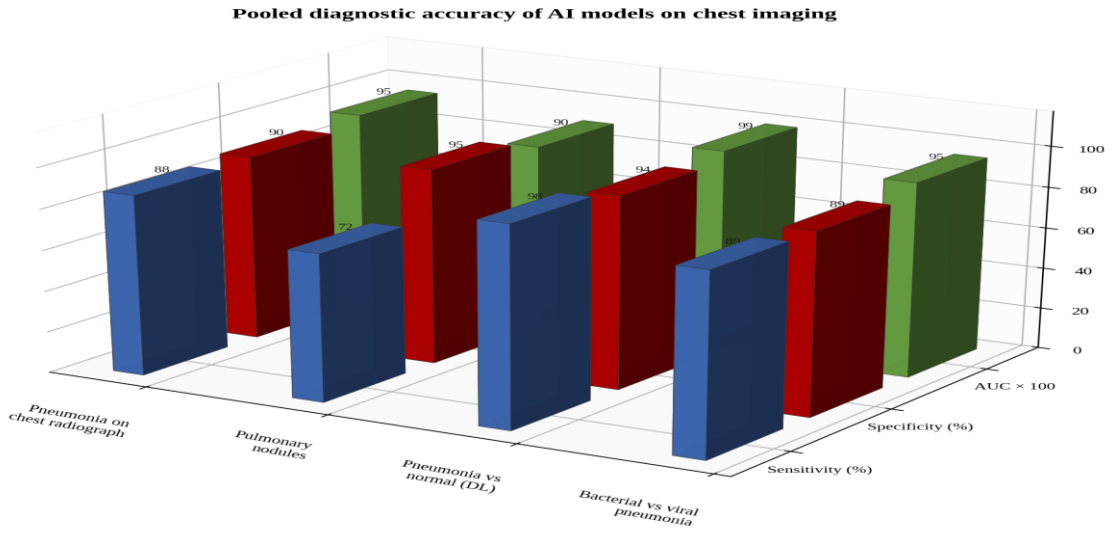

Figure 6. Pooled diagnostic accuracy of artificial-intelligence models on chest imaging (sensitivity, specificity and AUC × 100). Data from [51, 52].

Finally, artificial intelligence has entered thoracic imaging. Pooled analyses report a sensitivity of about 88% and specificity of about 90% (AUC ≈ 0.95) for pneumonia detection on chest radiographs, and about 72% sensitivity with 95% specificity (AUC ≈ 0.90) for pulmonary nodules; deep-learning meta-analyses report still higher pooled figures for discriminating pneumonia from normal radiographs (sensitivity 0.98, specificity 0.94, AUC 0.99) and for distinguishing bacterial from viral pneumonia (sensitivity and specificity 0.89, AUC 0.95) [51, 52]. Crucially, using such systems as a second reader improves radiologist sensitivity by roughly 9–10 percentage points [51]. These accuracies are summarised in Figure 6. Two caveats apply directly to the present context: external validation studies consistently show diminished performance on datasets from other institutions and populations [53], and no model has been trained or validated specifically on the imaging signature of CO-induced lung injury.

Table 6.

Diagnostic modalities for acute carbon monoxide poisoning and its pulmonary complications

Modality	What it measures	Strengths	Limitations
Arterial blood gas with co-oximetry	COHb fraction, PaO_2, $PaCO_2$, acid–base status	Reference standard; quantifies hypoxaemia and acidosis	Invasive; COHb falls rapidly with oxygen therapy [46]
Pulse CO-oximetry	Non-invasive COHb estimate	Rapid, bedside, useful for triage	Reduced accuracy with poor perfusion or motion; not recommended for diagnosis [34, 46]
Conventional pulse oximetry	SpO_2	Universally available	Cannot distinguish COHb from O_2Hb; falsely reassuring [46, 47]
Serum lactate	Anaerobic metabolism	Severity and prognosis marker	Non-specific; influenced by seizures and shock [35, 47]
Chest radiography / CT	Ground-glass density, cuffing, alveolar oedema, consolidation	Defines pattern and extent of pulmonary involvement	Abnormal in only ~1/3 of severe cases; non-specific [23, 24]
DLCO	Alveolar–capillary gas transfer	Functional correlate of alveolar destruction and membrane damage	Uses CO as test gas; confounded by residual COHb and anaemia [50]
Histology, morphometry, IHC	Septal thickness, airspace area, CD68, caspase-3	Objective, quantitative, phase-specific	Requires tissue; not standardised for CO [21, 42–44]
AI-assisted image analysis	Automated detection and classification	High pooled accuracy; improves reader sensitivity by 9–10 points	Performance falls on external datasets; not validated for CO [51–53]

4. Discussion

4.1. Coherence of the evidence

Three independent lines of evidence converge. Forensic series establish that pulmonary oedema, haemorrhage, congestion and emphysematous change are present in the great majority of fatal cases and that their severity is not predictable from COHb [25, 27]. Clinical and radiological series establish that subclinical pulmonary involvement is far commoner than overt respiratory failure, and that a minority of patients progress to acute respiratory distress syndrome [23, 32–35]. Experimental work establishes both the acute ultrastructural and permeability changes [20, 31] and, more recently, the durable emphysematous remodelling that persists six weeks after a single exposure [21]. Population-level cohort data close the loop by showing an increased subsequent risk of lung disease in survivors [22]. The agreement between species, settings and methods is strong enough to support a general model.

4.2. A two-phase morphogenetic model

The evidence is best organised as a two-phase, partially overlapping sequence. The first phase, occupying roughly the first 24 hours, is vascular–exudative. Its drivers are hydrostatic (congestion, stasis, venular obstruction) and permeability-related (oxidative damage to the alveolar–capillary barrier, endothelial and epithelial swelling, basement-membrane denudation). Its morphological signature is uniform septal thickening, protein-rich intra-alveolar transudate, diapedetic haemorrhage, bronchiolar spasm with epithelial desquamation and mucous plugging, and alternating atelectasis and acute local emphysema. Its histochemical signature is diffuse, moderate alcian-blue positivity in septa and perivascular stroma. Its immunohistochemical signature is a sharp rise in CD68 with, in young organisms, a parallel rise in caspase-3. Its morphometric signature is the maximum deviation of every index — septal thickness, airspace area, bronchiolar and arteriolar wall thickness.

The second phase, extending from the second day to at least six weeks, is inflammatory–destructive–reparative. Exudate is resorbed; macrophage-driven clearance and apoptotic elimination of damaged cells dominate; the protease–antiprotease and TGF-β axes determine whether the outcome is

restitution or remodelling. Its morphological signature is irregular septal thickening with focal rupture and coalescence of airspaces, diffuse bronchiolar desquamation, peribronchial infiltration, emphysematous enlargement and, where repair fails, focal fibrosis. Its histochemical signature is either bright focal alcian-blue positivity in new matrix (successful repair) or a weak, patchy reaction (failing repair). Its immunohistochemical signature is declining but still elevated CD68 with caspase-3 now exceeding it.

This model accounts for an otherwise puzzling observation in the forensic literature: the negative correlation between oedema and congestion on the one hand and emphysematous change on the other, reported by Pehlivan et al. [25]. If the exudative and the destructive patterns belong to different phases, then a lung dominated by one will tend not to be dominated by the other, and the negative correlation becomes an expected consequence of the time elapsed between exposure and death rather than an anomaly. The same reasoning explains the negative correlation between COHb and pneumonia or bronchitis: infective complications require survival, and survival permits COHb elimination [25].

4.3. Morphometry and immunohistochemistry as the missing link

The descriptive literature on CO lung pathology is rich but largely qualitative, and qualitative categories cannot support comparison across studies, across ages or across time points. Morphometry supplies that comparability. The data presented here show that the alveolar septum thickens by approximately 19–21% within six hours and remains 8–9% above control at one week; that the airspace area moves reciprocally; and that bronchiolar and arteriolar walls follow the same trajectory with slower normalisation. These are exactly the kinds of numbers that permit a pathologist to state how severe an injury is and how old it is, rather than merely that it is present.

Immunohistochemistry supplies the mechanistic dimension. The pairing of CD68 with caspase-3 is particularly informative because the two markers dissociate in time and this dissociation is itself diagnostic. An early CD68 peak with a low caspase-3 identifies the reactive phase; a declining CD68 with a rising caspase-3 identifies the destructive phase. A single section stained for both therefore carries information about the interval since exposure that no conventional stain provides — a property of obvious forensic value. The observation that caspase-3 induction is deferred in older animals adds a further dimension, since it implies that the same marker profile means different things at different ages.

4.4. Clinical and forensic implications

Four practical implications follow. First, because COHb predicts neither clinical severity nor pulmonary morphology, a normal or rapidly falling COHb should never be taken to exclude significant lung injury; assessment must be independent [25, 46]. Second, because subclinical radiographic involvement is roughly five times commoner than overt pulmonary oedema, chest imaging should be considered in severe poisoning even without respiratory symptoms, and ground-glass density should be read as a marker of significant hypoxaemia [23]. Third, because a single acute exposure produces emphysematous remodelling that persists for at least six weeks in experimental animals and is associated with increased chronic lung disease in human cohorts, survivors of severe poisoning warrant respiratory follow-up, ideally including diffusing capacity, in the same way that they are followed for delayed neuropsychiatric sequelae [21, 22, 50]. Fourth, in forensic practice, the combination of morphometric indices with CD68 and caspase-3 offers a means of estimating the interval between exposure and death and of distinguishing acute exudative from delayed destructive injury — information that cannot be obtained from COHb or from haematoxylin–eosin alone.

4.5. Gaps in the evidence and directions for future work

Several gaps are conspicuous. There is no standardised morphometric protocol for CO-induced lung injury, and consequently no reference ranges; the mean linear intercept has been reported at a single time point in a single study [21]. There are no published CD68 or caspase-3 data for the CO-poisoned lung, so the marker behaviour described here must be regarded as preliminary and requires independent replication. The age-dependence of the response has not been systematically studied, despite the fact that mortality is concentrated in older people. The relationship between the experimental emphysematous phenotype and human DLCO in survivors has not been tested, although the measurement is widely available. Serum KL-6, which rose in the experimental model [21], has not

been evaluated as a clinical marker of alveolar injury after CO poisoning. Finally, artificial-intelligence image analysis has never been trained on CO-specific findings, and its documented loss of accuracy on external datasets [53] means that models developed on Western cohorts cannot be assumed to transfer to Central Asian practice without local validation. Each of these represents a tractable research question.

4.6. Limitations of this review

This is a narrative and not a systematic review; it did not follow a registered protocol, and it is subject to selection and language bias despite the inclusion of Russian- and Uzbek-language sources. Quantitative pooling was precluded by the heterogeneity of species, exposure protocols, severity and observation intervals, so the numerical values presented illustrate direction and magnitude rather than pooled estimates. Several key ultrastructural and permeability findings derive from studies performed decades ago with methods that would not be used today, although they have not been contradicted by more recent work. The morphometric and immunohistochemical data in Figures 4 and 5 and Tables 4 and 5 are the authors' own preliminary results and have not yet been independently replicated. Finally, extrapolation from rodent to human lung must be cautious, since alveolar dimensions, collateral ventilation and the anatomy of the respiratory bronchiole differ between species.

Conclusion

Acute carbon monoxide poisoning injures the lung in a reproducible, staged and quantifiable manner. An early vascular–exudative phase — microcirculatory congestion and stasis, increased alveolar–capillary permeability, interstitial and alveolar oedema, diapedetic haemorrhage, bronchiolar epithelial desquamation and alternating atelectasis and acute emphysema — gives way, in those who survive, to a delayed inflammatory–destructive phase in which macrophage-driven inflammation, apoptosis, extracellular-matrix remodelling, emphysematous alveolar destruction and focal fibrosis predominate. Pulmonary oedema, emphysematous change and haemorrhage are the commonest findings at autopsy, and they correlate poorly with blood carboxyhaemoglobin, which means the lung must be assessed on its own morphological terms.

Morphometry of the alveolar septum, alveolar airspace, bronchiole and arteriole converts these descriptions into comparable numbers, and the paired immunohistochemical markers CD68 and caspase-3 separate the inflammatory from the cell-death component and, through their temporal dissociation, carry information about the interval since exposure. Age modifies both the severity and the sequence of these changes: in young organisms inflammation and apoptosis are activated together and recovery is comparatively complete, whereas in older organisms the early response is predominantly macrophagic, apoptosis is deferred and more intense, and structural normalisation is slower and incomplete.

The practical consequence is that the morphological evaluation of the lung after carbon monoxide poisoning should be standardised around a defined set of morphometric indices assessed together with CD68 and caspase-3 immunohistochemistry and alcian-blue histochemistry, and that survivors of severe poisoning deserve respiratory follow-up on the same footing as neurological follow-up. Establishing reference ranges for these indices, replicating the marker dynamics independently, and testing their correspondence with diffusing capacity in human survivors are the priorities for the next stage of research.

LIST OF REFERENCES:

1. GBD 2021 Carbon Monoxide Poisoning Collaborators. Global, regional, and national mortality due to unintentional carbon monoxide poisoning, 2000–2021: results from the Global Burden of Disease Study 2021. Lancet Public Health. 2023;8(11). doi:10.1016/S2468-2667(23)00185-8.
2. Wang W, Ling Y, Xiong X, Zhou J, Peña-Fernández A. Global patterns and trends of carbon monoxide poisoning: a comprehensive spatiotemporal analysis using joinpoint regression and ARIMA modeling, 1990–2021. PLoS One. 2025;20(8). doi:10.1371/journal.pone.0330778.
3. Yu Y, Yu J, Yuan D, Yang F, Yan H, Jiang P, et al. The burden of carbon monoxide poisoning in China from 1990 to 2021 and forecasts to 2050. Front Public Health. 2025;13:1642416. doi:10.3389/fpubh.2025.1642416.

4. Hampson NB. U.S. mortality due to carbon monoxide poisoning, 1999–2014: accidental and intentional deaths. Ann Am Thorac Soc. 2016;13(10):1768-1774. doi:10.1513/AnnalsATS.201604-318OC.
5. Can G, Sayılı U, Aksu Sayman Ö, et al. Mapping of carbon monoxide related death risk in Turkey: a ten-year analysis based on news agency records. BMC Public Health. 2019;19(1):9.
6. Braubach M, Algoet A, Beaton M, Lauriou S, Héroux ME, Krzyzanowski M. Mortality associated with exposure to carbon monoxide in WHO European Member States. Indoor Air. 2013;23(2):115-125. doi:10.1111/ina.12007.
7. Savioli G, Gri N, Ceresa IF, Piccioni A, Zanza C, Longhitano Y, et al. Carbon monoxide poisoning: from occupational health to emergency medicine. J Clin Med. 2024;13(9):2466. doi:10.3390/jcm13092466.
8. Rose JJ, Wang L, Xu Q, McTiernan CF, Shiva S, Tejero J, et al. Carbon monoxide poisoning: pathogenesis, management, and future directions of therapy. Am J Respir Crit Care Med. 2017;195(5):596-606. doi:10.1164/rccm.201606-1275CI.
9. Reumuth G, Alharbi Z, Houschyar KS, Kim BS, Siemers F, Fuchs PC, et al. Carbon monoxide intoxication: what we know. Burns. 2019;45(3):526-530. doi:10.1016/j.burns.2018.07.006.
10. Dent MR, Rose JJ, Tejero J, Gladwin MT. Carbon monoxide poisoning: from microbes to therapeutics. Annu Rev Med. 2024;75:337-351. doi:10.1146/annurev-med-052422-020045.
11. Kleinman MT. Carbon monoxide. In: Environmental Toxicants: Human Exposures and Their Health Effects. Hoboken: Wiley; 2020. p. 455-486.
12. Salthammer T. Carbon monoxide as an indicator of indoor air quality. Environ Sci Atmos. 2024;4(3):291-305. doi:10.1039/D4EA00006D.
13. Motterlini R, Foresti R. Biological signaling by carbon monoxide and carbon monoxide-releasing molecules. Am J Physiol Cell Physiol. 2017;312(3). doi:10.1152/ajpcell.00360.2016.
14. Ryter SW, Ma KC, Choi AMK. Carbon monoxide in lung cell physiology and disease. Am J Physiol Cell Physiol. 2018;314(2). doi:10.1152/ajpcell.00022.2017.
15. Hess DR. Inhaled carbon monoxide: from toxin to therapy. Respir Care. 2017;62(10):1333-1342. doi:10.4187/respcare.05781.
16. Zhang J, Piantadosi CA. Mitochondrial oxidative stress after carbon monoxide hypoxia in the rat brain. J Clin Invest. 1992;90(4):1193-1199. doi:10.1172/JCI115980.
17. Thom SR, Bhopale VM, Fisher D, Zhang J, Gimotty P. Delayed neuropathology after carbon monoxide poisoning is immune-mediated. Proc Natl Acad Sci U S A. 2004;101(37):13660-13665. doi:10.1073/pnas.0405642101.
18. Piantadosi CA, Zhang J, Levin ED, Folz RJ, Schmechel DE. Apoptosis and delayed neuronal damage after carbon monoxide poisoning in the rat. Exp Neurol. 1997;147(1):103-114. doi:10.1006/exnr.1997.6584.
19. Fisher AB, Hyde RW, Baue AE, Reif JS, Kelly DE. Effect of carbon monoxide on function and structure of the lung. J Appl Physiol. 1969;26(1):4-12. doi:10.1152/jappl.1969.26.1.4.
20. Niden AH, Schulz H. The ultrastructural effects of carbon monoxide inhalation on the rat lung. Virchows Arch Pathol Anat Physiol Klin Med. 1965;339:283-292.
21. Lee SJ, Kim T, Cha YS, Kim M, Lee JY, Lee WY. Alveolar damage and development of emphysema in rats with carbon monoxide poisoning. Mol Cell Toxicol. 2024;20(4):959-968.
22. Lee SJ, Lee S, Kim YH, Cha YS. Risk of lung diseases in patients with previous carbon monoxide poisoning: a nationwide population-based cohort study in the Republic of Korea. Clin Toxicol (Phila). 2024;62(7):425-431. doi:10.1080/15563650.2024.2371020.
23. Sone S, Higashihara T, Kotake T, Morimoto S, Miura T. Pulmonary manifestations in acute carbon monoxide poisoning. Am J Roentgenol Radium Ther Nucl Med. 1974;120(4):865-871. doi:10.2214/ajr.120.4.865.
24. Kittredge RD. Pulmonary edema in acute carbon monoxide poisoning. Am J Roentgenol Radium Ther Nucl Med. 1971;113(4):680-681. doi:10.2214/ajr.113.4.680.
25. Pehlivan S, Alacam H, Samdanci E, Kara D, Turkkan D, Altuntas A, et al. Evaluation of lung, cardiac and brain pathologies of death cases caused by carbon monoxide poisoning. Austin J Clin Neurol. 2016;3(1):1085.

26. Enikeev DA, et al. Structural and functional changes of the brain, lungs and heart in rats poisoned with carbon monoxide against a background of alcohol intoxication. Sovremennye Problemy Nauki i Obrazovaniya. 2021;(5):95. Russian.
27. Finck PA. Exposure to carbon monoxide: review of the literature and 567 autopsies. Mil Med. 1966;131(12):1513-1539.
28. Akyol S, Erdogan S, Idiz N, Celik S, Kaya M, Ucar F, et al. The role of reactive oxygen species and oxidative stress in carbon monoxide toxicity: an in-depth analysis. Redox Rep. 2014;19(5):180-189. doi:10.1179/1351000214Y.0000000094.
29. Bauer I, Pannen BH. Bench-to-bedside review: carbon monoxide - from mitochondrial poisoning to therapeutic use. Crit Care. 2009;13(4):220. doi:10.1186/cc7887.
30. Indiaminov SI, Kim AA. Manifestations of patho- and thanatogenesis in brain structures in carbon monoxide poisoning. Meditsinskie Novosti. 2020;(8):67-69. Russian.
31. Fein A, Grossman RF, Jones JG, Hoeffel J, McKay D. Carbon monoxide effect on alveolar epithelial permeability. Chest. 1980;78(5):726-731. doi:10.1378/chest.78.5.726.
32. Jang JH, Jang HJ, Kim HK, et al. Acute respiratory distress syndrome caused by carbon monoxide poisoning and inhalation injury recovered after extracorporeal membrane oxygenation along with direct hemoperfusion with polymyxin B-immobilized fiber column: a case report. J Med Case Rep. 2021;15:456. doi:10.1186/s13256-021-03023-w.
33. Chou CH, Ho CH, Weng CF, et al. Predicting duration of mechanical ventilation in patients with carbon monoxide poisoning: a retrospective study. J Crit Care. 2014;29(6):1130.e1-1130.e5.
34. American College of Emergency Physicians Clinical Policies Subcommittee (Writing Committee) on Carbon Monoxide Poisoning, Shih RD, Tomaszewski CA, Kaji A, Diercks DB, et al. A critical issue in the management of adult patients presenting to the emergency department with acute carbon monoxide poisoning: approved by the ACEP Board of Directors January 22, 2025. Ann Emerg Med. 2025;85(4). doi:10.1016/j.annemergmed.2024.12.005.
35. Anand J, Pawlas N, Schetz D, Kot J. Management of acute intoxication with carbon monoxide - Polish Medical Society, Section of Clinical Toxicology position statement. Int J Occup Med Environ Health. 2025;38(5):457-473. doi:10.13075/ijomeh.1896.02653.
36. Karapirli M, Kandemir E, Akyol S, Kantarci MN, Kaya M, Akyol O. Forensic and clinical carbon monoxide (CO) poisonings in Turkey: a detailed analysis. J Forensic Leg Med. 2013;20(2):95-101. doi:10.1016/j.jflm.2012.04.031.
37. Uysal C, Celik S, Duzgun Altuntas A, Kandemir E, Kaya M, Karapirli M, et al. Carbon monoxide-related deaths in Ankara between 2001 and 2011. Inhal Toxicol. 2013;25(2):102-106. doi:10.3109/08958378.2012.760020.
38. Xu W, Zhang Y, Wang J, et al. Carbon monoxide ameliorates lipopolysaccharide-induced acute lung injury via inhibition of alveolar macrophage pyroptosis. Exp Anim. 2023;72(1):77-87. doi:10.1538/expanim.22-0023.
39. Li W, Wang J, Chen Y, et al. Carbon monoxide attenuates lipopolysaccharide-induced acute lung injury in neonatal rats via downregulation of Cx43 to reduce necroptosis. Med Sci Monit. 2019;25:6255-6263.
40. Niu R, Cheng J, Sun J, Li F, Fang H, Lei R, et al. Alveolar type II cell damage and Nrf2-SOD1 pathway downregulation are involved in PM2.5-induced lung injury in rats. Int J Environ Res Public Health. 2022;19(19):12893. doi:10.3390/ijerph191912893.
41. Xodjiyev F, Hasanova D. Correction and histomorphological analysis of morphological changes in the gastric mucosa caused by chronic exposure to carbon monoxide. South Aral Region Medical Journal. 2025;1(4):235-241. Uzbek.
42. Ziablitsev DS, Kozyk M, Strubchevska K, Dyadyk OO, Ziablitsev SV. Lung expression of macrophage markers CD68 and CD163, angiotensin converting enzyme 2 (ACE2), and caspase-3 in COVID-19. Medicina (Kaunas). 2023;59(4):714.
43. Tu Z, Guo H, Gao Y, Xiao W, Xie X, Yu H, et al. Macrophage pyroptosis mediates hyperoxia-induced inflammatory lung injury in neonates. Front Immunol. 2025;16:1546986. doi:10.3389/fimmu.2025.1546986.

44. Xiao J, Wang L, Zhang B, Hou A. Cell death in acute lung injury: caspase-regulated apoptosis, pyroptosis, necroptosis, and PANoptosis. Front Pharmacol. 2025;16:1559659. doi:10.3389/fphar.2025.1559659.
45. Dong S, Zhang X, Yu JB, Li XY, Gong LR, Shi J, et al. Carbon monoxide attenuates lipopolysaccharide-induced lung injury by mitofusin proteins via p38 MAPK pathway. J Surg Res. 2018;228:201-210. doi:10.1016/j.jss.2018.03.042.
46. Goldin J, Cascella M. Diffusing capacity of the lungs for carbon monoxide. In: StatPearls [Internet]. Treasure Island (FL): StatPearls Publishing; 2024.
47. Aykut A, Günsoy E, Karabulut BÖ, et al. Serum lactate and carboxyhemoglobin as predictors of hyperbaric oxygen therapy in carbon monoxide poisoning: a retrospective study. BMC Emerg Med. 2025;25:252. doi:10.1186/s12873-025-01410-w.
48. Ho YW, Chung PY, Hou SK, Chang ML, Kang YN. Should we use hyperbaric oxygen for carbon monoxide poisoning management? A network meta-analysis of randomized controlled trials. Healthcare (Basel). 2022;10(7):1311. doi:10.3390/healthcare10071311.
49. Fujita M, Todani M, Ajimi Y, Yatabe T, Yokobori S, Araki M, et al. Evaluating the efficacy of hyperbaric oxygen therapy for acute carbon monoxide poisoning: a systematic review and meta-analysis. Acute Med Surg. 2026;13(1). doi:10.1002/ams2.70114.
50. Neder JA, Berton DC, Muller PT, O'Donnell DE. Incorporating lung diffusing capacity for carbon monoxide in clinical decision making in chest medicine. Clin Chest Med. 2019;40(2):285-305. doi:10.1016/j.ccm.2019.02.005.
51. Diagnostic accuracy of AI in chest radiography for pneumonia and lung cancer: a meta-analysis. Intell Based Med. 2025;12:100281.
52. Li Y, Zhang Z, Dai C, Dong Q, Badrigilan S. Accuracy of deep learning for automated detection of pneumonia using chest X-ray images: a systematic review and meta-analysis. Comput Biol Med. 2020;123:103898. doi:10.1016/j.compbiomed.2020.103898.
53. Yu AC, Mohajer B, Eng J. External validation of deep learning algorithms for radiologic diagnosis: a systematic review. Radiol Artif Intell. 2022;4(3). doi:10.1148/ryai.210064.

Entered 20.07.2026